ORIGINAL ARTICLE

Microbial dormancy improves development and experimental validation of ecosystem model

Gangsheng Wang[1,2], Sindhu Jagadamma[1,2], Melanie A Mayes[1,2], Christopher W Schadt[2,3], J Megan Steinweg[2,3,4], Lianhong Gu[1,2] and Wilfred M Post[1,2]

[1]Environmental Sciences Division, Oak Ridge National Laboratory, Oak Ridge, TN, USA; [2]Climate Change Science Institute, Oak Ridge National Laboratory, Oak Ridge, TN, USA and [3]Biosciences Division, Oak Ridge National Laboratory, Oak Ridge, TN, USA

Climate feedbacks from soils can result from environmental change followed by response of plant and microbial communities, and/or associated changes in nutrient cycling. Explicit consideration of microbial life-history traits and functions may be necessary to predict climate feedbacks owing to changes in the physiology and community composition of microbes and their associated effect on carbon cycling. Here we developed the microbial enzyme-mediated decomposition (MEND) model by incorporating microbial dormancy and the ability to track multiple isotopes of carbon. We tested two versions of MEND, that is, MEND with dormancy (MEND) and MEND without dormancy (MEND_wod), against long-term (270 days) carbon decomposition data from laboratory incubations of four soils with isotopically labeled substrates. MEND_wod adequately fitted multiple observations (total C–CO$_2$ and ^{14}C–CO$_2$ respiration, and dissolved organic carbon), but at the cost of significantly underestimating the total microbial biomass. MEND improved estimates of microbial biomass by 20–71% over MEND_wod. We also quantified uncertainties in parameters and model simulations using the Critical Objective Function Index method, which is based on a global stochastic optimization algorithm, as well as model complexity and observational data availability. Together our model extrapolations of the incubation study show that long-term soil incubations with experimental data for multiple carbon pools are conducive to estimate both decomposition and microbial parameters. These efforts should provide essential support to future field- and global-scale simulations, and enable more confident predictions of feedbacks between environmental change and carbon cycling.

Introduction

Climate change is expected to alter carbon cycle feedbacks from soils through shifts in the composition and carbon accrual rates of plants and microbes, as well as the magnitude and sign of nutrient fluxes (Manzoni et al., 2008; Melillo et al., 2011; Zhou et al., 2012; Weedon et al., 2013). However, these feedbacks are not yet predictable because we lack both mechanistic understanding and appropriate model structure. Theoretical analyses have been developed to account for the roles of microbes and/or exoenzymes in decomposition of litter and soil organic matter (SOM; for example, Schimel and Weintraub, 2003; Lawrence et al., 2009; Allison et al., 2010; Davidson et al., 2012; Moorhead et al.,

2012; Wang et al., 2013). Observations suggest that a critical parameter, the microbial carbon use efficiency (CUE) or microbial growth efficiency, is likely to decrease as a function of warming (Devevre and Horwath, 2000; Manzoni et al., 2008; Steinweg et al., 2008), which may result in lower microbial biomass, lower enzyme production and reduced heterotrophic respiration rates (Bradford et al., 2008; Hartley and Ineson, 2008; Tucker et al., 2013; Wang et al., 2013). These changes can occur either through physiological adjustments in individual microbial species/populations, for example, microbial CUE, or through shifts in the microbial community composition that change overall soil community CUE, or complex combinations thereof (Manzoni et al., 2012; Zhou et al., 2012). When the response of CUE to temperature change is not considered in models, soil carbon losses become magnified over time with warming (Frey et al., 2013; Wieder et al., 2013). When temperature-modified CUE is included, acclimation of the community to warmer temperatures moderates soil carbon loss (Sierra et al., 2010; Wieder et al., 2013), which is consistent with some experimental observations

(Frey *et al.*, 2008; Zhou *et al.*, 2012). The ability to understand the activities of microbes in response to climate change and perturbations appears to be key to predicting carbon cycle–climate feedbacks.

Microbially controlled SOM decomposition is increasingly represented in ecosystem models (Treseder *et al.*, 2012). Other vital common evolutionary traits, however, such as microbial dormancy and community shifts are not yet represented (Jones and Lennon, 2010; Weedon *et al.*, 2013). When environmental conditions are unfavorable for growth, microbes may enter a state of low metabolic activity until conditions improve to allow replication (Stolpovsky *et al.*, 2011; Wang *et al.*, 2014b). Failure to consider dormancy in microbially controlled decomposition could result in underestimate of microbial biomass. Alternatively, measurements of microbial biomass such as chloroform fumigation and quantitative polymerase chain reaction cannot readily inform microbial models unless the extent of dormancy is considered (Wang *et al.*, 2014b). Although soil respiration data are the most available and reliable observations for calibration and validation of models from point to global scale (Raich and Schlesinger, 1992; Hanson *et al.*, 2000), estimates of microbial biomass, and even stoichiometry, will ultimately be needed to parameterize microbial ecosystem models (Sinsabaugh *et al.*, 2013; Xu *et al.*, 2013).

Microbial SOM decomposition models contain two major categories of parameters: decomposition parameters and microbial parameters. Microbial parameters are related to microbial growth and maintenance and include maximum specific growth and maintenance rates, true growth yield (Y_G) and the half-saturation constant for microbial uptake (Wang *et al.*, 2014b). Our previous work has modified the microbial parameters using the physiological model to account for the extent of dormant versus active microbes (Wang *et al.*, 2014b). Short-term (that is, several days) substrate-induced respiration and substrate-induced growth response experiments can be used to estimate many microbial parameters (Van de Werf and Verstraete, 1987; Colores *et al.*, 1996; Blagodatskaya and Kuzyakov, 2013). However, the short-term nature of these experiments means that decomposition parameters for many slowly decomposing substrates cannot be estimated from them (Wang *et al.*, 2014b). Decomposition parameters refer to the kinetic parameters directly controlling decomposition rates, for example, rate constants in first-order kinetic models (Lawrence *et al.*, 2009), enzyme kinetics (maximum specific enzyme activity and corresponding half-saturation constant), and enzyme production and turnover rates (Schimel and Weintraub, 2003; Tang and Riley, 2013; Wang *et al.*, 2013).

In this study, we incorporated the dormant and active microbial physiological model developed in Wang *et al.* (2014b) into the microbial enzyme-mediated decomposition (MEND) model that represents the microbial enzyme-driven biological processes as well as the mineral-associated physicochemical processes (Wang *et al.*, 2013). Carbon isotopes were also represented in MEND to distinguish fluxes of native SOM from added ^{14}C-labeled substrates, thus providing additional data for model parameterization (Hanson *et al.*, 2005; Thiet *et al.*, 2006; Parton *et al.*, 2010). We tested two versions of MEND, that is, MEND with dormancy (hereinafter referred to as MEND) and MEND without dormancy (hereinafter referred to as MEND_wod), against C decomposition data collected from long-term laboratory incubations of soils with isotopically labeled substrate additions. We hypothesized that (i) MEND would be superior to MEND_wod to more accurately estimate microbial and SOM dynamics; (ii) long-term (~ 1 year) soil incubation experiments with observations of diverse response variables (for example, respiration, microbial biomass, dissolved organic carbon (DOC) and C isotopes) are useful for estimating decomposition parameters in addition to microbial parameters.

Materials and methods

MEND model accounting for microbial dormancy
We divided the microbial biomass pool in original MEND (MEND_wod) into two fractions, that is, active and dormant microbial biomass (BA and BD; Figure 1 for model diagram). The microbial physiology component was incorporated into MEND to account for the transition of microbes between the two physiological states (active and dormant; Wang *et al.*, 2014b). The particulate organic carbon (POC) pool may be divided into several sub-pools representing different substrate categories. For example, as per our laboratory experiments with addition of glucose and starch, we divided the POC pool into two components: POC_1 (denoted by P_1) containing lignocellulose-like compounds and POC_2 (denoted by P_2) including starch-like compounds. P_1 is degraded by ligninases and cellulases (Wang *et al.*, 2012; Li *et al.*, 2013), and P_2 is broken down by amylases (Caldwell, 2005; Swarbreck *et al.*, 2011). The DOC (D) pool contains compounds of varying complexity that can be bound to active layer of mineral-associated organic carbon (MOC, M) pool, that is, the Q pool in Figure 1 (Mayes *et al.*, 2012; Wang *et al.*, 2013). In MEND, the DOC (D) pool receives inputs from decomposition of POC (P) and MOC (M), desorption of C from Q, and dead enzymes and microbes (microbial biomass carbon, MBC).

The dynamics of each soil C pool in MEND is described by Supplementary Equations S1–S12 in the Supplementary Information. The transformation fluxes (Figure 1) are elucidated by Supplementary Equations S13–S26 in Supplementary Table S1 in the Supplementary Information. Model parameters and their *a priori* value ranges adapted from Wang *et al.* (2013) are summarized in Table 1.
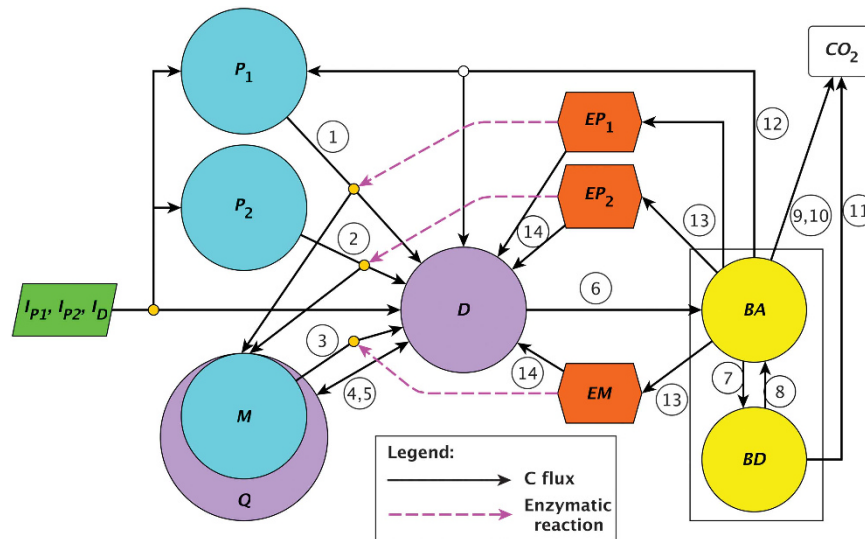
Figure 1 Diagram of the microbial ezyme-mediated decomposition (MEND) model. Soil organic carbon pools include: particulate organic carbon (POC) (for example, lignocellulose-like compounds and starch-like compounds, denoted by P_1 and P_2, respectively), mineral-associated organic carbon (MOC, denoted by M), dissolved organic carbon (DOC, D), adsorbed phase of DOC (QOC, Q), active microbial biomass (BA), dormant microbial biomass (BD), POC-degraded enzymes (for example, EP_1 and EP_2 that break down P_1 and P_2, respectively), and MOC-degraded enzymes (EM). I_{P1}, I_{P2} and I_D are external inputs to the pools of P_1, P_2, and D, respectively. Transformation fluxes include: (1) POC_1 (P_1) decomposition (denoted by the flux F_1 in equations in the Supplementary Information); (2) POC_2 (P_2) decomposition (F_2); (3) MOC (M) decomposition (F_3); (4, 5) adsorption (F_4) and desorption (F_5) between DOC (D) and QOC (Q); (6) DOC (D) uptake by BA (F_6); (7,8) dormancy (F_7) and reactivation (F_8) between BA and BD; (9, 10) BA growth respiration (F_9) and maintenance respiration (F_{10}); (11) BD maintenance respiration (F_{11}); (12) BA mortality (F_{12}); (13) synthesis of EP_1 ($F_{13,EP1}$), EP_2 ($F_{13,EP2}$), and EM ($F_{13,EM}$); and (14) turnover of enzymes ($F_{14,EP1}$, $F_{14,EP2}$, and $F_{14,EM}$).

There are two additional parameters for model initialization: initial active fraction (r_0) and initial lignocellulose fraction (LCF$_0$; Table 1). r_0 is the initial fraction of active microbes within total living microbes (Wang *et al.*, 2014b). LCF$_0$ is defined as the initial ratio of particulate lignocellulose–carbon (P_1) concentration to the total POC concentration. We define an index $\alpha = m_R/(V_D + m_R)$, where V_D and m_R denote maximum specific growth and maintenance rates, respectively, for active microbes. Either m_R or α is included in model calibration, as one of them can be derived from the other. Similarly, the binding affinity (K_{BA}) and desorption rate (K_{des}) are calibrated, and the specific adsorption rate ($K_{ads} = K_{des} \times K_{BA}$) can be computed from them. In MEND, the ratio of dormant to active maintenance rate is set to a constant (that is, $\beta = 0.001$), as the model is not sensitive to β during the experimental period (for example, within 1 year; Wang *et al.*, 2014b). Compared with MEND_wod, there is one more parameter in MEND—the initial active fraction (r_0). In summary, there are 20 parameters for calibrating MEND and 19 for MEND_wod.

Discriminating isotopes in the MEND model
The MEND and MEND_wod models were also modified to explicitly account for different C isotopes (for example, ^{12}C, ^{13}C and ^{14}C), that is, the soil C pools and fluxes represented in Figure 1 were duplicated to consider different C isotopes. General assumptions for the isotopically explicit MEND models include: (i) isotopic fractionation in SOM transformation, microbial processing and respiration is negligible (Sala *et al.*, 2000; Currie, 2007); (ii) each pool is mixed well and isotopically homogeneous, and influxes to a pool can alter its isotopic ratio, whereas outfluxes from a pool cannot (Currie, 2007). In this study, two C isotopes (^{14}C and ^{12}C) were included, and the flux of ^{14}C or ^{12}C is assumed to depend on the isotopic ratio (^{14}C/^{12}C) in the upstream pool.

$$F_{^{14}C} = \frac{R_{up}}{R_{up} + 1} \cdot F_C \qquad (1a)$$

$$F_{^{12}C} = \frac{1}{R_{up} + 1} \cdot F_C \qquad (1b)$$

where $F_{^{14}C}$ and $F_{^{12}C}$ represent the ^{14}C and ^{12}C flux, respectively; F_C is the total C flux; and $R_{up} = (^{14}C/^{12}C)_{up}$ denotes the isotopic ratio (^{14}C/^{12}C) in the upstream pool.

Model parameter optimization
We used the SCEUA (Shuffled Complex Evolution at University of Arizona) algorithm (Duan *et al.*, 1992; Wang *et al.*, 2009) to determine model parameters. We implemented SCEUA with 30 different random seeds (Duan *et al.*, 1992). The parameter optimization is to minimize the total objective function (J)

Table 1 MEND model parameters

Parameters	Description	A priori range	Eq.	Units
V_{P_1}	Maximum specific decomposition rate for P_1	(0.1, 3)	S13	$mg\,C\,mg^{-1}\,C\,h^{-1}$
V_{P_2}	Maximum specific decomposition rate for P_2	(1, 50)	S14	$mg\,C\,mg^{-1}\,C\,h^{-1}$
K_{P_1}	Half-saturation constant for P_1 decomposition	(1, 100)	S13	$mg\,C\,g^{-1}$ soil
K_{P_2}	Half-saturation constant for P_2 decomposition	(1, 100)	S14	$mg\,C\,g^{-1}$ soil
V_M	Maximum specific decomposition rate for M	(0.05, 2)	S15	$mg\,C\,mg^{-1}\,C\,h^{-1}$
K_M	Half-saturation constant for M decomposition	(10, 1000)	S15	$mg\,C\,g^{-1}$ soil
V_D	Maximum specific uptake rate of D for growth	(0.0001, 0.5)	S18	$mg\,C\,mg^{-1}\,C\,h^{-1}$
K_D	Half-saturation constant for uptake of D	(0.05, 0.5)	S18	$mg\,C\,g^{-1}$ soil
m_R	Specific maintenance rate of $BA = V_D \times \alpha/(1-\alpha)$		S18	$mg\,C\,mg^{-1}\,C\,h^{-1}$
α	$= m_R/(V_D + m_R)$	(0.01, 0.5)		—
β	Ratio of dormant maintenance rate to m_R	0.001	S23	—
Y_G	True growth yield	(0.1, 0.9)	S18	—
f_D	Fraction of decomposed P_1 and P_2 allocated to D	(0.1, 1)	S3	—
g_D	Fraction of dead BA allocated to D	(0.01, 1)	S1	—
p_{EP}	Fraction of m_R for production of EP_1 and EP_2	(0.001, 0.1)	S25	—
p_{EM}	Fraction of m_R for production of EM	(0.001, 0.1)	S25	—
r_E	Turnover rate of EP_1, EP_2 and EM	(0.0001, 0.01)	S26	$mg\,C\,mg^{-1}\,C\,h^{-1}$
Q_{max}	Maximum DOC sorption capacity	(0.5, 5)	S16	$mg\,C\,g^{-1}$ soil
K_{BA}	Binding affinity	(1, 16)		$(mg\,C\,g^{-1}$ soil$)^{-1}$
K_{des}	Desorption rate	(0.0001, 0.1)	S17	$mg\,C\,g^{-1}$ soil h^{-1}
K_{ads}	Specific adsorption rate $= K_{des} \times K_{BA}$		S16	$mg\,C\,mg^{-1}\,C\,h^{-1}$
LCF_0	Initial fraction of $P_1 = P_1/(P_1 + P_2)$	(0.1, 0.95)		—
r_0	Initial active fraction $= BA/(BA + BD)$	(0.01, 1)		—

Abbreviations: BA and BD, active and dormant microbial biomass; DOC, dissolved organic carbon; Eq., equations; LCF, lignocellulose fraction; MEND, microbial enzyme-mediated decomposition; Y_G, true growth yield.
Notes: The column 'Eq' lists the major equation nos. (see Supplementary Information) in which each parameter is used.

that is computed as the weighted average of multiple single-objectives (Wang and Chen, 2012)

$$J = \sum_{i=1}^{m} w_i \cdot J_i \qquad (2a)$$

$$\sum_{i=1}^{m} w_i = 1 \text{ with } w_i \in [0,1] \qquad (2b)$$

where m denotes the number of objectives and w_i is the weighting factor for the ith ($i = 1, 2,\ldots, m$) objective (J_i).

In this study, the total objective function (J) consists of four single-objectives (that is, $m = 4$) in terms of four response variables: J_1 for total cumulative respiration (denoted by C–CO$_2$), J_2 for cumulative respired ^{14}C normalized by added ^{14}C (denoted by %^{14}C–CO$_2$), J_3 for MBC and J_4 for DOC. The computation of each single-objective includes the data from two experiments (with addition of glucose and starch). For example, we merged the respiration data with glucose addition (number of data points $n = 14$) and the respiration data from starch ($n = 14$) into one data set ($n = 28$) for computing J_1.

The objectives J_1 (for C–CO$_2$) and J_2 (for %^{14}C–CO$_2$) were computed as $(1 - R^2)$, where R^2 denotes the coefficient of determination (Devore, 2008), and higher R^2-values ($R^2 \leqslant 1$) indicate better model performance; while the objectives J_3 and J_4 (for MBC and DOC, respectively) were calculated by the mean absolute relative error (MARE) and lower MARE values (MARE $\geqslant 0$) are preferred (Dawson et al., 2007). We used a different formulation for J_1

and J_2 from J_3 and J_4 because we had more observations for C–CO$_2$ and %^{14}C–CO$_2$ ($n = 28$ with glucose and starch for each of them) than for MBC and DOC ($n = 8$ for each of them). R^2 is not suitable for assessing the goodness-of-fit regarding a small amount of data. MARE represents the averaged deviations of predictions (Y_{sim}) from their observations (Y_{obs}):

$$MARE = \frac{1}{n}\sum_{i=1}^{n}\left|\frac{Y_{sim}(i) - Y_{obs}(i)}{Y_{obs}(i)}\right| \qquad (3)$$

Uncertainty and statistical analyses
The uncertainties in parameters and model predictions were quantified by the Critical Objective Function Index (COFI) method, which is much simpler than the commonly used method based on Bayesian inference and Markov Chain Monte Carlo (Wang and Chen, 2013). The COFI method is based on a global stochastic optimization technique (for example, SCEUA in this study). It also accounts for model complexity (represented by the number of model parameters) and observational data availability (represented by the number of observations).

The procedure of COFI includes: (i) implementing the SCEUA algorithm with multiple different random seeds to search 'relatively optimal' parameter sets that minimizing the objective function (J in Equation (2)); (ii) collecting the optimal parameter set generated in each loop of the SCEUA searching process to form a feasible parameter space; (iii) determining the COFI (J_{cr}; see Equation (4) below)

based on J_{opt} (minimum J-value), n (number of measurements) and p (number of model parameters); (iv) constructing the parametric surface of the confidence space by selecting those parameter sets resulting in $J \leqslant J_{cr}$ from the feasible parameter space; (v) quantifying the uncertainty in parameters by the statistics of these selected parameter sets; (vi) conducting model simulations using these selected parameter sets; and (vii) quantifying the uncertainty in model predictions (for example, soil C pool sizes and respiration) using the model simulation outputs.

The COFI is computed as (Batstone *et al.*, 2003; Wang *et al.*, 2014a):

$$J_{cr} = J_{opt} \cdot \eta = J_{opt} \cdot \left(1 + \frac{p}{n-p} F_{\alpha, p, n-p}\right) \quad (4)$$

where J_{cr} is the COFI that defines the parameter uncertainty region, J_{opt} is the optimum (minimum) objective function value that is calculated by Equation (2a), n is the number of measured data points, p is the number of parameters, and $F_{\alpha, p, n-p}$ is the value of the F-distribution for α, p and $n-p$. For MEND, $P = 20$, $n = 72$ (including measured C–CO$_2$, %^{14}C–CO$_2$, DOC and MBC in two experiments with addition of glucose and starch), we used $\alpha = 0.05$, with $F_{0.05, 20, 52} = 1.776$ to estimate the 95% confidence parameter uncertainty regions. For MEND_wod, $P = 19$ (that is, r_0 is not included) and $F_{0.05, 19, 53} = 1.786$. As a result, $\eta = 1.683$ and 1.640 for MEND and MEND_wod, respectively. It is evident that more observed data points and less undetermined parameters would reduce parametric uncertainty (that is, smaller J_{cr}).

We used the non-parametric Kruskal–Wallis analysis of variance to test whether the parameter samples for each soil originated from the same distribution at a significance level of 0.05 (McDonald, 2009; Giraudoux, 2013).

Soils and incubation experiments
We have chosen to study four soils selected from contrasting climatic zones, the experimental details of which were published previously: A Gelisol from arctic, Andisol from sub-arctic, Mollisol from temperate, as well as an Ultisol from tropical regions (Jagadamma *et al.*, 2014a, b). In brief, each soil was incubated at room temperature (20 °C) for 270 days in the dark in a temperature and humidity controlled room. For each sample, 25 g soil were pre-incubated at 40% water holding capacity for 1 week to avoid the respiration response of the microbial community to rewetting (Paul *et al.*, 2001; Haddix *et al.*, 2011). Each soil sample was amended with unlabeled substrate (D-glucose or starch) at the concentration of 0.4 mg C g^{-1} soil and with uniformly labeled ^{14}C substrates (U-^{14}C glucose or U-^{14}C starch). The added glucose and starch were assumed to enter the DOC (D) and POC_starch (P_2) pool, respectively. The initial conditions of soils are

summarized in Table 2. The initial Q pool size was assumed to be 1% of the MOC (M) pool size and the initial enzyme concentrations for EP$_1$, EP$_2$ and EM were set to 1.1×10^{-3}, 1.1×10^{-3} and 1.4×10^{-3} mg C g^{-1} soil, respectively (Wang *et al.*, 2013). The radiocarbon labeled glucose and starch were added to soils that had isotopic ratios ($R = {}^{14}$C/^{12}C) of 4.80×10^{-6} (for glucose) and 4.68×10^{-6} (for starch), respectively. Cumulative total respiration (denoted by C–CO$_2$ in units of mg C g^{-1} soil) and cumulative respired ^{14}C normalized by added ^{14}C (denoted by %^{14}C–CO$_2$) were measured 14 times in three replicates, that is, at days of 1, 2, 4, 6, 10, 15, 30, 45, 60, 90, 120, 150, 210 and 270. In addition, MBC and DOC were determined at 4 days, that is, 4, 30, 150 and 270. Additional details about the soils and the laboratory-incubation experiments can be found in Jagadamma *et al.* (2014a, b).

Results

Model simulations
Both MEND and MEND_wod could simulate the observed C–CO$_2$, %^{14}C–CO$_2$ and DOC with similarly satisfactory criterion values (Figures 2a, b and d). Higher R^2-values ($R^2 \leqslant 1$) indicate better model performance, whereas lower MARE values (MARE $\geqslant 0$) are preferred. The R^2-values for C–CO$_2$ and %^{14}C–CO$_2$ are > 0.85 and close to the ideal R^2-value (1.0). The MARE values for DOC are < 0.32 with most of them < 0.20 for both models. For MBC, the MARE values for MEND_wod are > 0.65 and are 25–126% higher than those for MEND (Figure 2c). MEND_wod underestimated 91% of the 32 MBC observations (eight observations for each of the four soils), whereas the MEND underestimated 75%. When dormancy was not considered, the MARE for MBC predictions averaged out to 0.70 during the full experimental period and 0.95 during the latter period (at days of 150 and 270). When dormancy was included, the average MARE values were reduced to 0.37 and 0.47 for the full period and the latter period, respectively. Thus, MEND improved model estimates of MBC concentrations by 20–71% over MEND_wod across four soils.

Taking the Mollisol as an example (Figure 3, the error bars for model simulations were derived by the COFI method), the simulated C–CO$_2$ (Figures 3a and c), %^{14}C–CO$_2$ (Figures 3b and d) and DOC (Figures 3f and h) by both models fit the observations very well. MEND_wod greatly underestimated %^{14}C–CO$_2$ during the first 2 days (see the left two points in Figures 3b and d) and slightly underestimated %^{14}C–CO$_2$ from days 2 to 15 (data point 3–6 in Figures 3b and d). However, MEND improved the estimates of %^{14}C–CO$_2$ for the same period. The simulated MBC concentrations (Figures 3e and g) by MEND were also close to the observations, while MEND_wod significantly underestimated MBC at

days 150 and 270. Similar results were found for the other soils (see Supplementary Figure S1 in the Supplementary Information).

Model parameters

The parameter analysis in this section is focused on MEND, as it represents microbial dynamics better and presents superior model performance than MEND_wod. The boxplots for model parameters derived by the COFI method are shown in Supplementary Figure S2 in the Supplementary Information. In most cases, the calibrated parameter values varied among soils. The Andisol held the highest values in seven parameters (r_E, V_{P2}, K_{P1}, K_M, Q_{max}, K_D and g_D) and the lowest in the other seven parameters (m_R, V_D, p_{EM}, V_{P1}, V_M, K_{P2}, K_{des}).

The decomposition parameters varied in different SOC pools (Supplementary Figure S2). The MOC (M) pool had the lowest maximum specific decomposition rate (median of $V_M = 0.93$, 95% confidence interval (CI) $= 0.06$–1.98 mg C mg^{-1} C h^{-1}) and the largest half-saturation constant (median of $K_M = 550$, 95% CI $= 35$–998 mg C g^{-1} soil). The P_2 pool (starch) held the highest specific decomposition rate (median of $V_{P2} = 42$, 95% CI $= 16$–50 mg C mg^{-1} C h^{-1}) and the lowest half-saturation constant (median of $K_{P2} = 6$, 95% CI $= 1$–56 mg C g^{-1} soil). The P_1 (lignocellulose) had slightly higher specific decomposition rate (median of $V_{P1} = 1.17$ mg C mg^{-1} C h^{-1}) than the M pool while having a modest half-saturation constant (median of $K_{P1} = 58$ mg C g^{-1} soil). Other decomposition parameters are related to the turnover and production of enzymes (r_E, p_{EP} and p_{EM}). The overall r_E (enzyme turnover rate) had a median of 0.003 with the 95% CI the same as the *a priori* (0.0001–0.01). The Gelisol exhibited the lowest median r_E (0.001). The distributions of r_E were not statistically different between the Mollisol and the Andisol (median $= 0.004$ and 0.005, respectively). The median r_E for the Ultisol (0.002) was between the previous two groups (Supplementary Figure S2). The fractions of m_R for the production of EP and EM (p_{EP} and p_{EM}) across four soils had medians of 0.06 and 0.04, respectively, with their 95% CIs almost identical to their *a priori* ranges.

Major microbial parameters in MEND include the specific maintenance and growth rates (m_R and V_D), the half-saturation constant for microbial uptake (K_D) and the Y_G. The medians of m_R and V_D for the four soils were 0.01 and 0.03 mg C mg^{-1} C h^{-1}, respectively, (Supplementary Figure S2). m_R and V_D were significantly different among the four soils with the highest in the Gelisol and the lowest in the Andisol. K_D exhibited a median of 0.467 (95% CI $= 0.09$–0.50 mg C g^{-1} soil). The overall Y_G had a median of 0.43 with 95% CI of 0.10–0.75 (Supplementary Figure S2). The medians (close to the means) for the Gelisol, Andisol, Mollisol and Ultisol were 0.25, 0.42, 0.49 and 0.52, respectively.

Discussion

Model parameterization

The Andisol stands out of the four soils in terms of model parameters because Andisols are different from other soil pertaining to their physical, chemical and mineralogical properties (Nanzyo, 2002; McDaniel and Wilson, 2007). The Andisol contained significantly higher SOC than the other soils (Table 2) but generally produced lower cumulative C–CO_2 than the Mollisol and Ultisol during the experimental period. Thus the model calibration required the lowest specific reaction rates (for example, m_R, V_D, V_{P1} and V_M) and the highest half-saturation constants (for example, K_{P1}, K_M and K_D) for the Andisol. The median values for m_R and V_D derived here are two orders of magnitude higher than those in Wang *et al.* (2013). This is because of the consideration of microbial dormancy. The MEND_wod model and other microbial models include only one microbial biomass pool and do not consider the physiological states of microbes. Thus, the m_R values in Wang *et al.* (2013) were summarized from literature including maintenance rates for active microbes (Anderson and Domsch, 1985b) or dormant microbes (Anderson and Domsch, 1985a) or the total microbial biomass. In MEND, m_R solely refers to the maximum specific maintenance rate of active microbes. The large differences in m_R and V_D between MEND and MEND_wod point to the importance of proper accounting in parameterization of microbial ecosystem models.

Our results showed the dependence of Y_G on the changes in temperature (ΔT in Figure 4), where ΔT is the difference between incubation temperature (20 °C) and the mean annual temperature (Table 2). Figure 4 shows that Y_G decreased with increasing ΔT from 0.7 to 22.9 °C. The temperature-response coefficient for Y_G (that is, the regression slope in Figure 4) was approximately -0.01 °C^{-1} with 95% CI of (-0.016 and -0.005) °C^{-1}, which comprises previous experimental estimates (Devevre and Horwath, 2000; Steinweg *et al.*, 2008; Tucker *et al.*, 2013). This dependence of Y_G on ΔT (Figure 4) may imply that microbes have been acclimated to their local environments and exhibit a relatively universal Y_G (averaged 0.56 with 95% CI of 0.48–0.64) across different biomes.

When observations are available for various response variables, the strategy of multi-objective calibration is essential in order to reduce uncertainty in model parameterization (Yapo *et al.*, 1998; Wang and Chen, 2012). We conducted model parameterization aiming at minimizing a synthesized objective function that consists of four objectives in terms of C–CO_2, %^{14}C–CO_2, DOC and MBC. The optimal parameter sets reflected a balance among all objectives. We also found that the parameterization results could be qualitatively different when a new objective was introduced into the

calibration process. Our previous study indicated that short-term substrate-induced respiration or substrate-induced growth response experiments could be used to determine microbial parameters (Wang *et al.*, 2014b). This study further shows that the long-term (that is, ~1 year) soil incubations or field experiments with measurements of microbial biomass in addition to soil respiration are conducive to estimate decomposition parameters in addition to microbial parameters. We also advocate the incorporation of isotopic signatures into parameterization and evaluation of ecosystem models. We have shown our efforts in parameterizing the model in terms of diverse soils from different climatic regions. We hope that these parameter values could provide documented references, although with large uncertainty, for relating parameters to soil properties and/or climatic conditions. Nevertheless, more laboratory- and field-scale data sets are needed to constrain model parameterization and associated uncertainty. By this way, the microbial mechanisms could be practically incorporated into ecosystem models to represent microbial-controlled processes.

Table 2 Experimental soils and their initial soil carbon pool sizes (mg C g^{-1} soil)

Soils	POC	MOC	DOC	MBC	Location	MAT
Gelisol	4.25	11.04	0.17	0.05	Fairbanks, AK, USA	−2.9
Andisol	20.06	64.86	0.64	0.86	Krýsuvíkurheiði, Reykjanes, Iceland	5.0
Mollisol	3.25	27.97	0.21	0.64	Batavia, IL, USA	11.3
Ultisol	4.71	17.67	0.48	0.52	Lavras, Minas Gerais, Brazil	19.3

Abbreviations: DOC, dissolved organic carbon; MAT, mean annual temperature (°C); MBC, microbial biomass carbon; MOC, mineral-associated organic carbon; POC, particulate organic carbon.

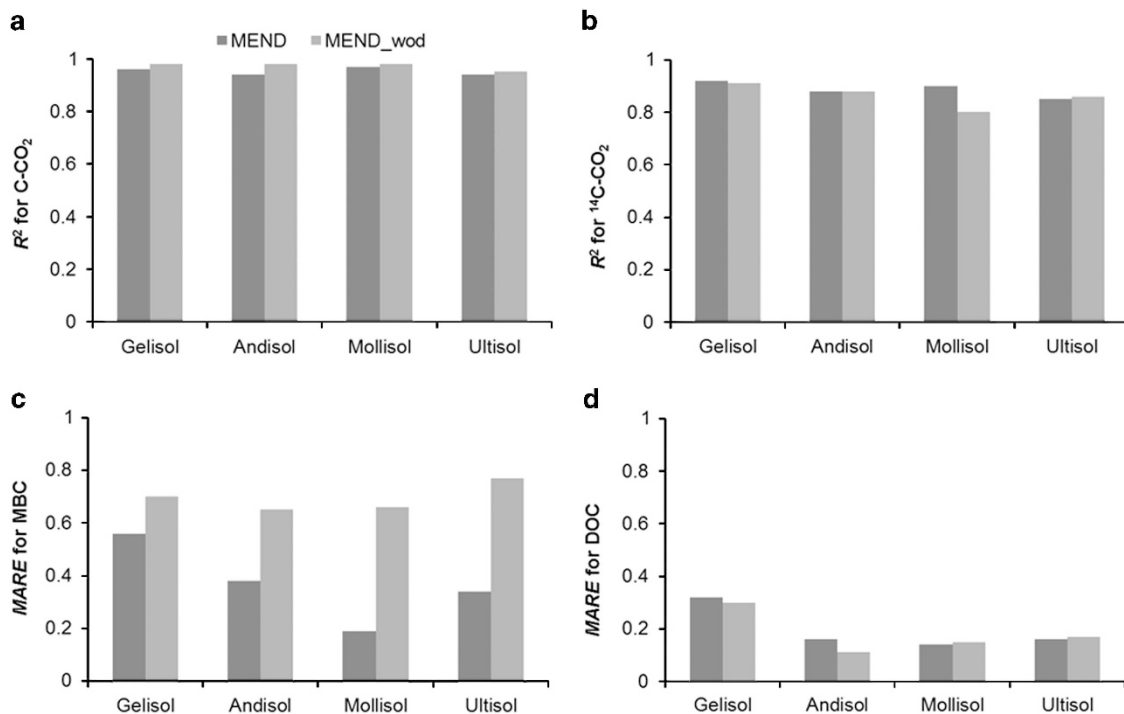**Figure 2** Best criterion values for calibrating MEND model with dormancy (MEND) or without dormancy (MEND_wod). (**a**) R^2 for C–CO$_2$ (cumulative C–CO$_2$ respiration); (**b**) R^2 for ^{14}C–CO$_2$ (normalized cumulative ^{14}C–CO$_2$ by added ^{14}C); (**c**) MARE for MBC (microbial biomass carbon); (**d**) MARE for DOC (dissolved organic carbon). R^2: coefficient of determination, higher R^2-values ($R^2 \leqslant 1$) indicate better model performance; MARE, mean absolute relative error (Equation (3)), lower MARE values (MARE $\geqslant 0$) are better.

Figure 3 Comparison between observations (Obs) and simulations (Sim) for the Mollisol, where 'MEND' and 'MEND_wod' denote the MEND model with and without dormancy, respectively. (**a**) C–CO$_2$ (cumulative C–CO$_2$ respiration) with addition of glucose. (**b**) %^{14}C–CO$_2$ (normalized cumulative respired ^{14}C by added ^{14}C) with glucose. (**c**) C–CO$_2$ with addition of starch. (**d**) %^{14}C–CO$_2$ with starch. (**e**) MBC (microbial biomass carbon) with glucose. (**f**) DOC (dissolved organic carbon) with glucose. (**g**) MBC with starch; (**h**) DOC with starch. The horizontal error bars in **a–d** are s.d. for observations (sample size $n = 3$) at days of 1, 2, 4, 6, 10, 15, 30, 45, 60, 90, 120, 150, 210 and 270 (from left to right); the vertical error bars in **a–d** are s.d. for C–CO$_2$ simulated by MEND ($n = 2346$); for clarity, the error bars (similar to MEND) by MEND_wod are not shown in **a–d**. No error bars are shown for observations in **e–h** because of the lack of replicate measurements. The error bars in **e–h** are s.d. for simulations; for clarity, only the positive errors are shown.
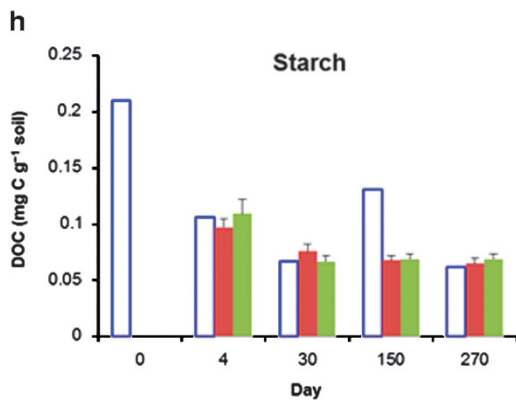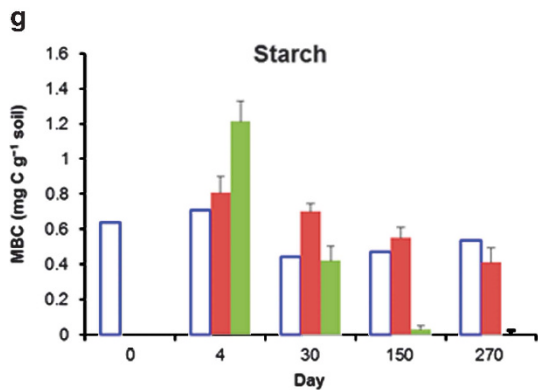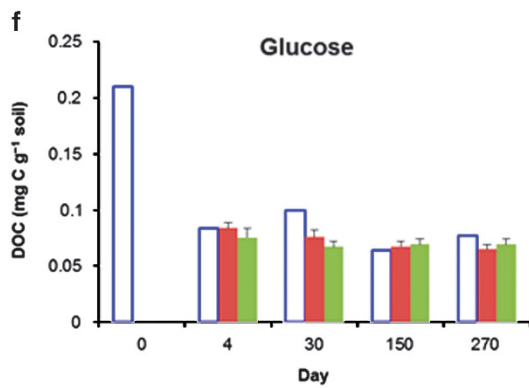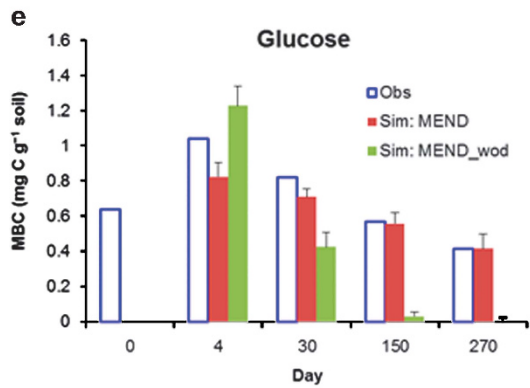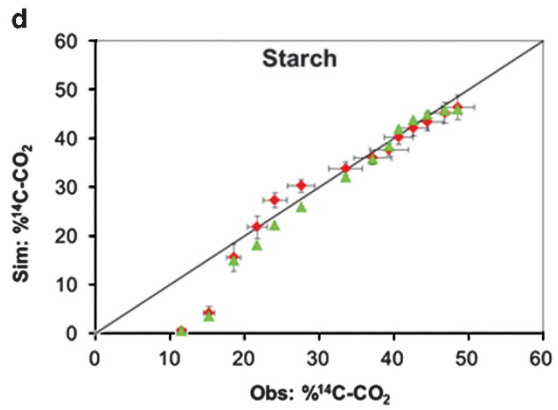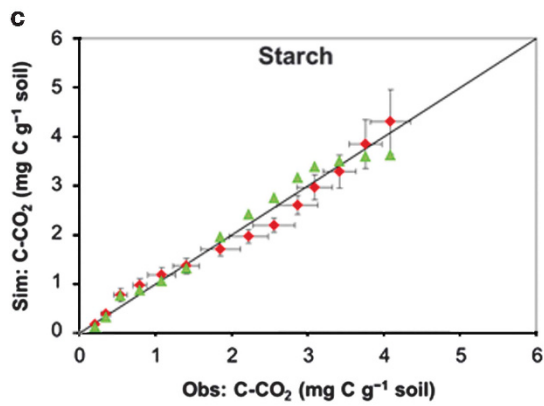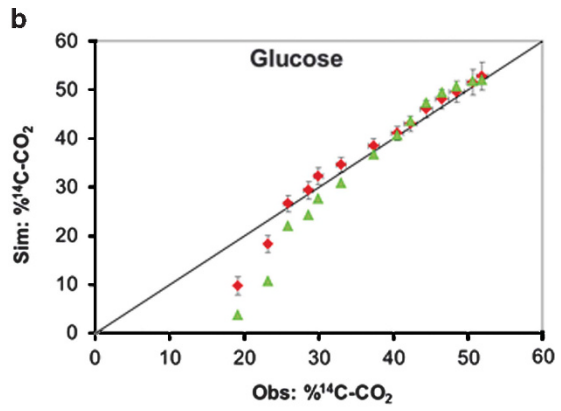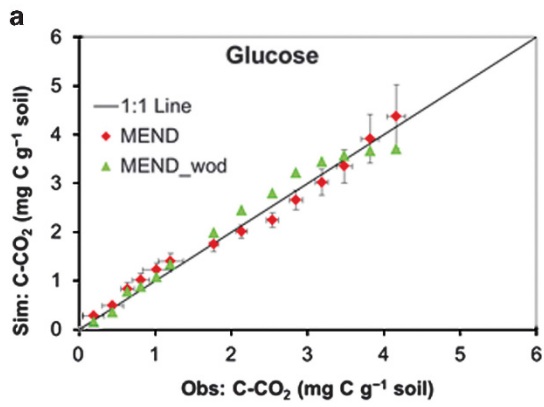
Microbial dormancy

The observations of low respiration rates but modest MBC and DOC concentrations during the latter period (for example, after 50 days) of incubation imply there must be certain mechanisms further depressing microbial activities. The total MBC or DOC usually exhibited a decreasing trend after 4 days, but MBC concentrations at day 150 were as high as 28–89% of initial MBC, and DOC concentrations were at least 30% of initial DOC. The lower microbial activities are reflected by the slower increase in cumulative C–CO_2 and ^{14}C–CO_2 (Figures 3a–d). That is why very low MBC concentrations (compared with initial MBC) were predicted with satisfactory predictions of DOC when MEND_wod was adopted (Figures 3e and g, and Supplementary Figure S1). Major factors affecting microbial activities include environmental factors (for example, soil temperature and moisture; Brockett *et al.*, 2012), carbon availability or root exudation (Drake *et al.*, 2013) and nutrient availability (Lennon and Jones, 2011). Changes in these factors might result in changes in CUE (Sinsabaugh *et al.*, 2013) and transitions between microbial physiological states (active and dormant), particularly in laboratory-scale experiments. For example, dormancy is a beneficial survival and evolutionary trait of soil microbes when faced with unfavorable environmental conditions (Lennon and Jones, 2011). The impacts of environmental factors and root exudation could be excluded from this study, as the soils without living roots were incubated at an aerobic environment with constant soil temperature and moisture. We found that the prediction of microbial biomass could not be improved by simply manipulating the intrinsic CUE (that is, Y_G) in MEND_wod. Thus, the transition between microbial physiological states owing to changes in carbon or nutrient availability is the most likely explanation for the observed variations in microbial activities.

The MEND model substantially improved the predictions of microbial biomass over MEND_wod, indicating that it is essential to represent dormancy in microbial ecosystem models in order to accurately predict microbial biomass as well as to explain variation in SOM decomposition as a function of time. The initial active fractions (r_0) in this study averaged 0.79 (median = 0.90) with large variations (95% CI = 0.19–0.99). The relatively high r_0 might be due to the pre-incubation of soil samples at 40% water holding capacity for 1 week. The active fraction (r) generally declined with time due to the decrease in substrate (DOC) availability. Taking the Mollisol as an example, the active fraction (r) dropped from its initial value of 0.655 to 0.104 after 50 days (Figure 5). At day 150, the predicted MBC concentrations by MEND_wod only accounted for 3–8% of the initial MBC across four soils, which were much lower than the observations (>28% of initial MBC). The incorporation of dormancy was able to resolve the large discrepancies in total MBC between model predictions and experimental observations.

MEND_wod could adequately fit the other observations (C–CO_2, %^{14}C–CO_2 and DOC), but at the cost of significantly underestimating the total microbial biomass. In other words, if the total microbial biomass could be more satisfactorily modeled, the model without dormancy would poorly simulate soil respiration, not to mention that microbial uptake and respiration are more sensitive to the changes in MBC than to the changes in DOC concentration regarding the Michaelis–Menten kinetics (Wang and Post, 2013). Taking the Mollisol as an example, when MBC was given greater weight in the objective function (Equation (2)) of MEND_wod, the best MARE for MBC could be improved from 0.66 (when soil respiration was given greater weight) to 0.27; however, the model was not good at simulating C–CO_2 (best $R^2 = 0.78$) compared with the model performance shown in Figure 2 (best $R^2 = 0.98$ for C–CO_2). In this MEND_wod configuration, the cumulative respiration at day 270 was overestimated by 29%, compared with the relative small errors of 5% from MEND. In conclusion, the inclusion of dormancy substantially improves the estimates of microbial biomass as well as the mechanistic representation and prediction of soil carbon cycle.

Feedbacks between the climate system and the carbon cycle is a major focus of global change research (Zhou *et al.*, 2012). Biogeochemical cycles including the carbon cycle are extensively driven by microbes (Falkowski *et al.*, 2008). The two necessary conditions for soil microbes to affect ecological processes are: (a) 'organisms must differ in their functional traits' and (b) 'biological reactions must be
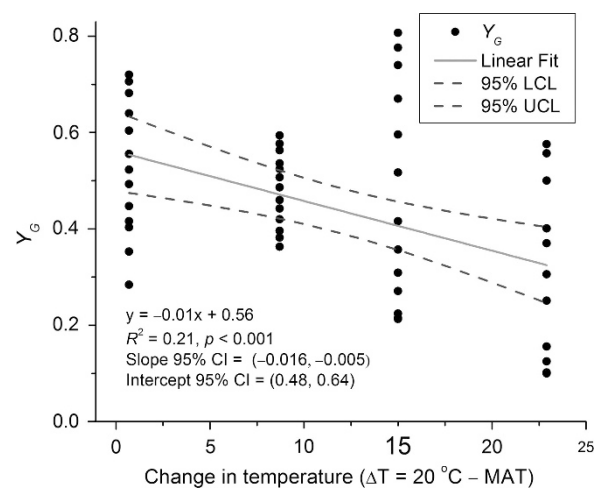

Figure 4 Dependence of true growth yield (Y_G) on changes in temperature. MAT, mean annual temperature at the soil sampling site; CI, confidence interval; LCL, and UCL are lower and upper confidence limits, respectively. The Y_G-values for each soil (from left to right: Ultisol, Mollisol, Andisol and Gelisol) are 13 representative values corresponding to 13 percentiles (2.5, 5, 10, 20, 30, 40, 50, 60, 70, 80, 90, 95 and 97.5%).
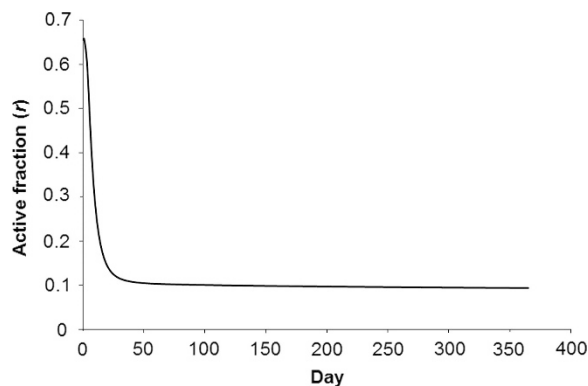
Figure 5 Temporal change in active fraction (r) of microbial biomass for the Mollisol.

either the rate-limiting step or the fate-controlling step' (Schimel and Schaeffer, 2012). Microbial functional groups are characterized by certain functional traits, such as life-history traits and substrate-specificity traits (Kaiser *et al.*, 2014). The newly developed microbial mineral carbon stabilization model defines two microbial functional groups (r- and K-strategies) that differ in growth rate, turnover rate and their interactions with physically and chemically protected SOM pools (Wieder *et al.*, 2014). Our model testing against experimental data demonstrates that the microbial control over SOM decomposition is substantial. In addition, active and dormant microbes distinctly differ in their functional traits, and the extent of microbial decomposition and uptake is the rate-limiting step.

The dormancy strategy should be more significant for microbes in field conditions that are influenced by carbon and nutrient availability and changes in environmental factors such as soil temperature, moisture and oxygen (Wang *et al.*, 2014b). For example, dormancy has been found to be a better strategy to achieve drought resistance in mineral soils where C supply constrains growth and osmolyte synthesis (Manzoni *et al.*, 2014). The proposed dormancy mechanism and calibrated microbial, and enzymatic parameters with long-term laboratory incubations provide a pathway forward for modeling field-scale processes. Although the importance of microbial community composition may vary with spatiotemporal scales (Schimel and Schaeffer, 2012), the inclusion of microbial physiology is essential to confidently project feedbacks between climate change and carbon cycle (Bradford, 2013). Continued development is needed to bring microbial physiology into global climate and ecosystem models (Todd-Brown *et al.*, 2012; Treseder *et al.*, 2012; Schimel, 2013).

Conflict of Interest

The authors declare no conflict of interest.

Disclaimer

References

Allison SD, Wallenstein MD, Bradford MA. (2010). Soil-carbon response to warming dependent on microbial physiology. *Nat Geosci* **3**: 336–340.

Anderson TH, Domsch KH. (1985a). Determination of ecophysiological maintenance carbon requirements of soil microorganisms in a dormant state. *Biol Fert Soils* **1**: 81–89.

Anderson TH, Domsch KH. (1985b). Maintenance carbon requirements of actively-metabolizing microbial populations under *in situ* conditions. *Soil Biol Biochem* **17**: 197–203.

Batstone DJ, Pind PF, Angelidaki I. (2003). Kinetics of thermophilic, anaerobic oxidation of straight and branched chain butyrate and valerate. *Biotechnol Bioeng* **84**: 195–204.

Blagodatskaya E, Kuzyakov Y. (2013). Active microorganisms in soil: Critical review of estimation criteria and approaches. *Soil Biol Biochem* **67**: 192–211.

Bradford MA. (2013). Thermal adaptation of decomposer communities in warming soils. *Front Microbiol* **4**: Article 333.

Bradford MA, Davies CA, Frey SD, Maddox TR, Melillo JM, Mohan JE *et al.* (2008). Thermal adaptation of soil microbial respiration to elevated temperature. *Ecol Lett* **11**: 1316–1327.

Brockett BF, Prescott CE, Grayston SJ. (2012). Soil moisture is the major factor influencing microbial community structure and enzyme activities across seven biogeoclimatic zones in western Canada. *Soil Biol Biochem* **44**: 9–20.

Caldwell BA. (2005). Enzyme activities as a component of soil biodiversity: A review. *Pedobiologia* **49**: 637–644.

Colores GM, Schmidt SK, Fisk MC. (1996). Estimating the biomass of microbial functional groups using rates of growth-related soil respiration. *Soil Biol Biochem* **28**: 1569–1577.

Currie WS. (2007). Modeling the dynamics of stable-isotope ratios for ecosystem biogeochemistry. In: Michener R, Lajtha K (eds) *Stable Isotopes in Ecology and Environmental Science*. Blackwell Publishing: Malden, MA, USA, pp 450–479.

236

Davidson EA, Samanta S, Caramori SS, Savage K. (2012). The Dual Arrhenius and Michaelis–Menten kinetics model for decomposition of soil organic matter at hourly to seasonal time scales. *Global Change Biol* **18**: 371–384.

Dawson CW, Abrahart RJ, See LM. (2007). HydroTest: a web-based toolbox of evaluation metrics for the standardised assessment of hydrological forecasts. *Environ Model Software* **22**: 1034–1052.

Devevre OC, Horwath WR. (2000). Decomposition of rice straw and microbial carbon use efficiency under different soil temperatures and moistures. *Soil Biol Biochem* **32**: 1773–1785.

Devore JL. (2008). *Probability and Statistics for Engineering and the Sciences*, 7th edn Brooks/Cole Cengage Learning: Florence, KY, USA.

Drake J, Darby B, Giasson M-A, Kramer M, Phillips R, Finzi A. (2013). Stoichiometry constrains microbial response to root exudation-insights from a model and a field experiment in a temperate forest. *Biogeosciences* **10**: 821–838.

Duan QY, Sorooshian S, Gupta V. (1992). Effective and efficient global optimization for conceptual rainfall-runoff models. *Water Resour Res* **28**: 1015–1031.

Falkowski PG, Fenchel T, Delong EF. (2008). The microbial engines that drive Earth's biogeochemical cycles. *Science* **320**: 1034–1039.

Frey S, Drijber R, Smith H, Melillo J. (2008). Microbial biomass, functional capacity, and community structure after 12 years of soil warming. *Soil Biol Biochem* **40**: 2904–2907.

Frey SD, Lee J, Melillo JM, Six J. (2013). The temperature response of soil microbial efficiency and its feedback to climate. *Nat Clim Change* **3**: 395–398.

Giraudoux P. (2013). R Package 'pgirmess': Data analysis in ecology, 1.5.8 edn.

Haddix ML, Plante AF, Conant RT, Six J, Steinweg JM, Magrini-Bair K *et al.* (2011). The role of soil characteristics on temperature sensitivity of soil organic matter. *Soil Sci Soc Am J* **75**: 56–68.

Hanson PJ, Edwards NT, Garten CT, Andrews JA. (2000). Separating root and soil microbial contributions to soil respiration: A review of methods and observations. *Biogeochemistry* **48**: 115–146.

Hanson PJ, Swanston CW, Garten C, Todd D, Trumbore SE. (2005). Reconciling change in Oi-horizon carbon-14 with mass loss for an oak forest. *Soil Sci Soc Am J* **69**: 1492–1502.

Hartley IP, Ineson P. (2008). Substrate quality and the temperature sensitivity of soil organic matter decomposition. *Soil Biol Biochem* **40**: 1567–1574.

Jagadamma S, Steinweg JM, Mayes MA, Post WM. (2014a). Substrate quality alters microbial mineralization of added substrate and soil organic carbon. *Biogeosci Discuss* **11**: 4451–4482.

Jagadamma S, Steinweg JM, Mayes MA, Wang G, Post WM. (2014b). Decomposition of added and native organic carbon from physically separated fractions of diverse soils. *Biol Fert Soils* **50**: 613–621.

Jones SE, Lennon JT. (2010). Dormancy contributes to the maintenance of microbial diversity. *Proc Natl Acad Sci* **107**: 5881–5886.

Kaiser C, Franklin O, Dieckmann U, Richter A. (2014). Microbial community dynamics alleviate stoichiometric constraints during litter decay. *Ecol Lett* **17**: 680–690.

Lawrence CR, Neff JC, Schimel JP. (2009). Does adding microbial mechanisms of decomposition improve soil organic matter models? A comparison of four models using data from a pulsed rewetting experiment. *Soil Biol Biochem* **41**: 1923–1934.

Lennon JT, Jones SE. (2011). Microbial seed banks: the ecological and evolutionary implications of dormancy. *Nat Rev Microbiol* **9**: 119–130.

Li J, Ziegler SE, Lane CS, Billings SA. (2013). Legacies of native climate regime govern responses of boreal soil microbes to litter stoichiometry and temperature. *Soil Biol Biochem* **66**: 204–213.

Manzoni S, Jackson RB, Trofymow JA, Porporato A. (2008). The global stoichiometry of litter nitrogen mineralization. *Science* **321**: 684–686.

Manzoni S, Schaeffer SM, Katul G, Porporato A, Schimel JP. (2014). A theoretical analysis of microbial eco-physiological and diffusion limitations to carbon cycling in drying soils. *Soil Biol Biochem* **73**: 69–83.

Manzoni S, Taylor P, Richter A, Porporato A, Ågren GI. (2012). Environmental and stoichiometric controls on microbial carbon-use efficiency in soils. *New Phytol* **196**: 79–91.

Mayes MA, Heal KR, Brandt CC, Phillips JR, Jardine PM. (2012). Relation between soil order and sorption of dissolved organic carbon in temperate subsoils. *Soil Sci Soc Am J* **76**: 1027–1037.

McDaniel P, Wilson M. (2007). Physical and chemical characteristics of ash-influenced soils of Inland Northwest forests. In: Page-Dumroese D, Miller R, Mital J, McDaniel P, Miller D (eds) *Volcanic-Ash-Derived Forest Soils of the Inland Northwest: Properties and Implications for Management and Restoration*. U.S. Department of Agriculture: Coeur d'Alene, ID, USA, pp 31–45.

McDonald JH. (2009). *Handbook of Biological Statistics* vol. 2. Sparky House Publishing: Baltimore, MD, USA.

Melillo JM, Butler S, Johnson J, Mohan J, Steudler P, Lux H *et al.* (2011). Soil warming, carbon–nitrogen interactions, and forest carbon budgets. *Proc Natl Acad Sci USA* **108**: 9508–9512.

Moorhead DL, Lashermes G, Sinsabaugh RL. (2012). A theoretical model of C-and N-acquiring exoenzyme activities, which balances microbial demands during decomposition. *Soil Biol Biochem* **53**: 133–141.

Nanzyo M. (2002). Unique properties of volcanic ash soils. *Global Environ Res-Eng Ed* **6**: 99–112.

Parton WJ, Hanson PJ, Swanston C, Torn M, Trumbore SE, Riley W *et al.* (2010). ForCent model development and testing using the Enriched Background Isotope Study experiment. *J Geophys Res Biogeosci* **115**: G04001.

Paul EA, Morris SJ, Böhm S. (2001). The determination of soil C pool sizes and turnover rates: biophysical fractionation and tracers. In: Lal R, Kimble JM, Follett RF, Stewart BA (eds) *Assessment Methods for Soil Carbon*. Lewis Publishers: Boca Raton, USA, pp 193–206.

Raich J, Schlesinger W. (1992). The global carbon dioxide flux in soil respiration and its relationship to vegetation and climate. *Tellus B* **44**: 81–99.

Sala OE, Jackson RB, Mooney HA, Howarth RW (eds) (2000). *Methods in Ecosystem Science*. Springer-Verlag: NY, USA, p 421.

Schimel JP. (2013). Microbes and global carbon. *Nat Clim Change* **3**: 867–868.

Schimel JP, Schaeffer SM. (2012). Microbial control over carbon cycling in soil. *Front Microbiol* **3**: Article 348.

Schimel JP, Weintraub MN. (2003). The implications of exoenzyme activity on microbial carbon and nitrogen limitation in soil: a theoretical model. *Soil Biol Biochem* **35**: 549–563.

Sierra J, Brisson N, Ripoche D, Déqué M. (2010). Modelling the impact of thermal adaptation of soil microorganisms and crop system on the dynamics of organic matter in a tropical soil under a climate change scenario. *Ecol Model* **221**: 2850–2858.

Sinsabaugh RL, Manzoni S, Moorhead DL, Richter A. (2013). Carbon use efficiency of microbial communities: stoichiometry, methodology and modelling. *Ecol Lett* **16**: 930–939.

Steinweg JM, Plante AF, Conant RT, Paul EA, Tanaka DL. (2008). Patterns of substrate utilization during long-term incubations at different temperatures. *Soil Biol Biochem* **40**: 2722–2728.

Stolpovsky K, Martinez-Lavanchy P, Heipieper HJ, Van Cappellen P, Thullner M. (2011). Incorporating dormancy in dynamic microbial community models. *Ecol Model* **222**: 3092–3102.

Swarbreck SM, Sudderth EA St, Clair SB, Salve R, Castanha C, Torn MS *et al.* (2011). Linking leaf transcript levels to whole plant analyses provides mechanistic insights to the impact of warming and altered water availability in an annual grass. *Global Change Biol* **17**: 1577–1594.

Tang JY, Riley WJ. (2013). A total quasi-steady-state formulation of substrate uptake kinetics in complex networks and an example application to microbial litter decomposition. *Biogeosciences* **10**: 8329–8351.

Thiet RK, Frey SD, Six J. (2006). Do growth yield efficiencies differ between soil microbial communities differing in fungal: bacterial ratios? Reality check and methodological issues. *Soil Biol Biochem* **38**: 837–844.

Todd-Brown KE, Hopkins FM, Kivlin SN, Talbot JM, Allison SD. (2012). A framework for representing microbial decomposition in coupled climate models. *Biogeochemistry* **109**: 19–33.

Treseder KK, Balser TC, Bradford MA, Brodie EL, Dubinsky EA, Eviner VT *et al.* (2012). Integrating microbial ecology into ecosystem models: challenges and priorities. *Biogeochemistry* **109**: 7–18.

Tucker CL, Bell J, Pendall E, Ogle K. (2013). Does declining carbon-use efficiency explain thermal acclimation of soil respiration with warming? *Global Change Biol* **19**: 252–263.

Van de Werf H, Verstraete W. (1987). Estimation of active soil microbial biomass by mathematical analysis of respiration curves: calibration of the test procedure. *Soil Biol Biochem* **19**: 261–265.

Wang G, Barber ME, Chen S, Wu JQ. (2014a). SWAT modeling with uncertainty and cluster analyses of tillage impacts on hydrological processes. *Stochastic Environ Res Risk Assess* **28**: 225–238.

Wang G, Chen S. (2012). A review on parameterization and uncertainty in modeling greenhouse gas emissions from soil. *Geoderma* **170**: 206–216.

Wang G, Chen S. (2013). Evaluation of a soil greenhouse gas emission model based on Bayesian inference and MCMC: Model uncertainty. *Ecol Model* **253**: 97–106.

Wang G, Mayes MA, Gu L, Schadt CW. (2014b). Representation of dormant and active microbial dynamics for ecosystem modeling. *PLoS One* **9**: e89252.

Wang G, Post WM. (2013). A note on the reverse Michaelis–Menten kinetics. *Soil Biol Biochem* **57**: 946–949.

Wang G, Post WM, Mayes MA. (2013). Development of microbial-enzyme-mediated decomposition model parameters through steady-state and dynamic analyses. *Ecol Appl* **23**: 255–272.

Wang G, Post WM, Mayes MA, Frerichs JT, Jagadamma S. (2012). Parameter estimation for models of ligninolytic and cellulolytic enzyme kinetics. *Soil Biol Biochem* **48**: 28–38.

Wang G, Xia J, Chen J. (2009). Quantification of effects of climate variations and human activities on runoff by a monthly water balance model: a case study of the Chaobai River basin in northern China. *Water Resour Res* **45**: W00A11.

Weedon JT, Aerts R, Kowalchuk GA, van Logtestijn R, Andringa D, van Bodegom PM. (2013). Temperature sensitivity of peatland C and N cycling: Does substrate supply play a role? *Soil Biol Biochem* **61**: 109–120.

Wieder W, Grandy A, Kallenbach C, Bonan G. (2014). Integrating microbial physiology and physiochemical principles in soils with the MIcrobial-MIneral Carbon Stabilization (MIMICS) model. *Biogeosci Discuss* **11**: 1147–1185.

Wieder WR, Bonan GB, Allison SD. (2013). Global soil carbon projections are improved by modelling microbial processes. *Nat Clim Change* **3**: 909–912.

Xu X, Thornton PE, Post WM. (2013). A global analysis of soil microbial biomass carbon, nitrogen and phosphorus in terrestrial ecosystems. *Global Ecol Biogeogr* **22**: 737–749.

Yapo PO, Gupta HV, Sorooshian S. (1998). Multi-objective global optimization for hydrologic models. *J Hydrol* **204**: 83–97.

Zhou J, Xue K, Xie J, Deng Y, Wu L, Cheng X *et al.* (2012). Microbial mediation of carbon-cycle feedbacks to climate warming. *Nat Clim Change* **2**: 106–110.

Supplementary Information accompanies this paper on The ISME Journal website (http://www.nature.com/ismej)